Applied Surface Science 255 (2008) 241–244

Contents lists available at ScienceDirect

Applied Surface Science

journal homepage: www.elsevier.com/locate/apsusc

Hydrogen-induced buckling of Pd films studied by positron annihilation

J. Čížek [a,*], I. Procházka [a], M. Vlach [a], N. Žaludová [a], S. Daniš [a], P. Dobroň [a], F. Chmelík [a], G. Brauer [b], W. Anwand [b], A. Mücklich [b], E. Nikitin [c], R. Gemma [c], R. Kirchheim [c], A. Pundt [c]

[a] Faculty of Mathematics and Physics, Charles University in Prague, V Holešovičkách 2, CZ-180 00 Praha 8, Czech Republic
[b] Institut für Ionenstrahlphysik und Materialforschung, Forschungszentrum Dresden-Rossendorf, Postfach 510119, D-01314 Dresden, Germany
[c] Institut fur Materialphysik, Universität Göttingen, Friedrich-Hund-Platz 1, D-37077 Göttingen, Germany

ARTICLE INFO

Article history:
Available online 23 May 2008

Keywords:
Palladium films
Hydrogen
Slow positron implantation spectroscopy
Acoustic emission
Transmission electron microscopy

ABSTRACT

Hydrogen loading of thin films introduces very high compressive stresses which grow in magnitude with increasing hydrogen concentration. When the hydrogen-induced stresses exceed a certain critical in-plane stress value, the loaded film starts to detach from the substrate. This results in the formation of buckles of various morphologies in the film layer. Defect studies of a hydrogen loaded Pd film which undergoes a buckling process are presented, using slow positron implantation spectroscopy, *in situ* acoustic emission, and direct observations of the film structure by transmission electron and optical microscopies. It is found that buckling of the film occurs at hydrogen concentrations $x_H \geq 0.1$ and causes a significant increase of the dislocation density in the film.

1. Introduction

Hydrogen dissolved in interstitial sites of a host metal causes a lattice expansion, which is isotropic in free standing bulk samples. However, in thin films the in-plane expansion is hindered by clamping of the film to the substrate. As a consequence, high compressive in-plane stresses up to several GPa may occur due to hydrogen loading [1]. These stresses grow with increasing hydrogen content, and when they exceed a certain critical in-plane stress they may cause local or global detachment of the loaded film. This detachment at the interface between the film and the substrate results in various buckling morphologies [2–6]. The hydrogen-induced buckling may cause adhesion failure in many thin film systems, but it can also be used to measure the adhesion energy between a metal film and a substrate [5]. The formation of buckles represents an irreversible change of film shape (i.e. plastic deformation) and should, therefore, proceed by generation and gliding of dislocations. Although the buckle morphology has been investigated in a number of works, detailed defect studies of the buckled films have, to the best of our knowledge, not been performed.

In the present work, defect studies of hydrogen loaded thin Pd films are reported. These defect studies were performed by slow positron implantation spectroscopy (SPIS) in combination with *in situ* acoustic emission (AE) measurements. Direct observations of the film structure were performed by transmission electron microscopy (TEM) and optical microscopy (OM).

2. Experimental details

Thin Pd films with a thickness of 1080 nm as determined by TEM (see Fig. 1a), were prepared in an UHV chamber (10^{-10} mbar) using cathode beam sputtering at room temperature on optically polished $(1\,1\,\bar{2}\,0)$ sapphire substrates. The samples were then step-by-step loaded with hydrogen by electrochemical charging [7] in a galvanic cell filled with a 1-M KOH electrolyte. The hydrogen concentration in the sample can be calculated from the Faraday's Law and is expressed as the atomic ratio H/Pd throughout this paper. SPIS studies of defects in thin films were performed at the magnetically guided positron beam "SPONSOR" [8] with a positron energy adjustable from 0.03 to 36 keV. Doppler broadening of the annihilation line was measured by a Ge detector with an energy resolution of (1.09 ± 0.01) keV at 511 keV and evaluated using the lineshape parameters. The energy window range for the *S* parameter calculation was (510.54, 511.46) keV. The AE studies were performed *in situ* during the step-by-step hydrogen loading of the films using a computer controlled DAKEL-XEDO-3 AE system to monitor AE on the basis of threshold-level detection, whereas the threshold voltage for the AE count was 480 mV (full scale was ±2.4 V). A piezoelectric

* Corresponding author at: Department of Low-Temperature Physics, Faculty of Mathematics and Physics, Charles University, V Holešovičkách 2, CZ-180 00, Praha 8, Czech Republic. Tel.: +420 2 21912788; fax: +420 2 2191 2567.
E-mail address: jakub.cizek@mff.cuni.cz (J. Čížek).

0169-4332/$ – see front matter © 2008 Elsevier B.V. All rights reserved.
doi:10.1016/j.apsusc.2008.05.290

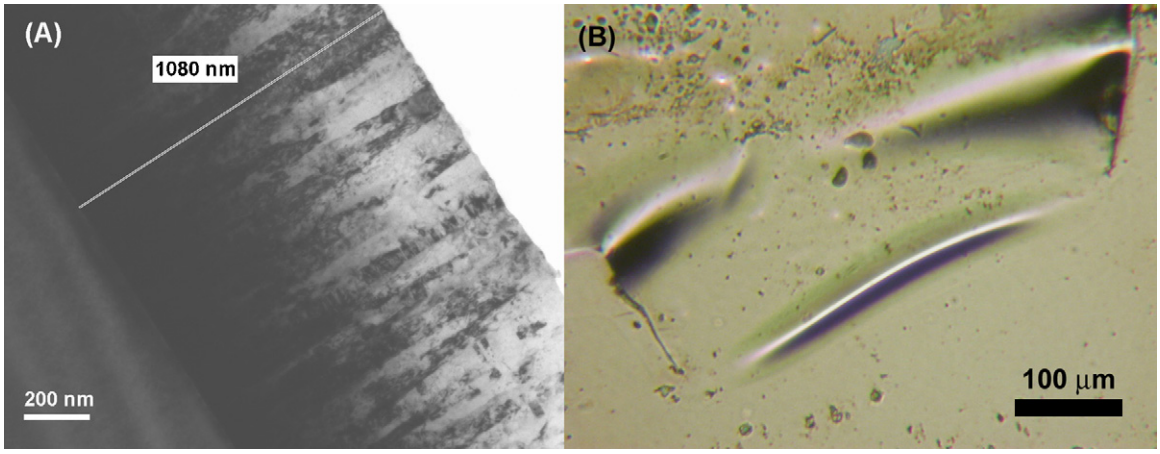

Fig. 1. (A) Bright field TEM image of the virgin film and (B) OM image of typical buckle morphology in the film loaded up to $x_H = 0.30$.

sensor MST8S (a frequency band from 100 to 600 kHz) was attached to the back side on the substrate of the loaded film, while the front side with the Pd film was immersed in the electrolyte. The TEM studies were performed with a Philips CM300SuperTWIN microscope operating at 300 kV. Thin foils for cross-sectional TEM were produced by conventional preparation using a Gatan precision ion polishing system (PIPS). An inverse metallographic microscope, Arsenal AM-2T, was used for the OM observations of the films.

3. Results and discussion

In Fig. 1, results of TEM and OM are presented. TEM revealed the presence of nanocrystalline "column-like" elongated grains with a lateral width around 50 nm in the virgin sample, whereas from OM the buckling due to hydrogen loading is clearly visible. In Fig. 2a, various $S(E)$ dependences representing different sample states are displayed. From the given thickness of the Pd film, i.e. 1080 nm as determined by TEM, it is certain that positron annihilation in the substrate is negligible up to an energy of 25 keV. All S parameters are normalized to the bulk $S_0 = 0.4968(7)$ value measured on a well-annealed reference bulk Pd sample. The $S(E)$ curve for the reference Pd sample is plotted in Fig. 2a as well. Fit of the curve by VEPFIT software (model 5 - S and diffusion length fitted independently, a single layer assumed) [9] gave a diffusion length of (151 ± 4) nm which can be considered as the mean diffusion length of free positrons in defect-free Pd. One can see in Fig. 2a that the film exhibits significantly higher S and shorter positron diffusion length compared to well-annealed bulk Pd. It is attributed to the nanocrystalline grain size which leads to a significant volume fraction of grain boundaries containing open-volume defects. The mean grain size in the film as estimated by TEM (see Fig. 1a) is three times smaller than the positron diffusion length in defect-free Pd, hence, most of thermalized positrons diffuse to grain boundaries and are trapped at open volume defects there. This leads to very short positron diffusion length and high S parameter values as observed for the film.

Selected $S(E)$ curves for the hydrogen loaded films are shown in Fig. 2a. They all can be well fitted by VEPFIT (see the solid lines in Fig. 2a) using a single layer model. The S parameter values S_{Pd} and the positron diffusion length $L_{+,Pd}$ for the Pd layer obtained from the fit are plotted in Fig. 2b. The vacancy-like open volume defects at grain boundaries do trap not only positrons, but also hydrogen atoms. Both experimental [10] and theoretical [11] investigations showed that hydrogen is not located in the centre of vacancy, but at certain distance away. It was proved that vacancies with attached hydrogen atoms are still able to trap positrons [12]. Hence, at low

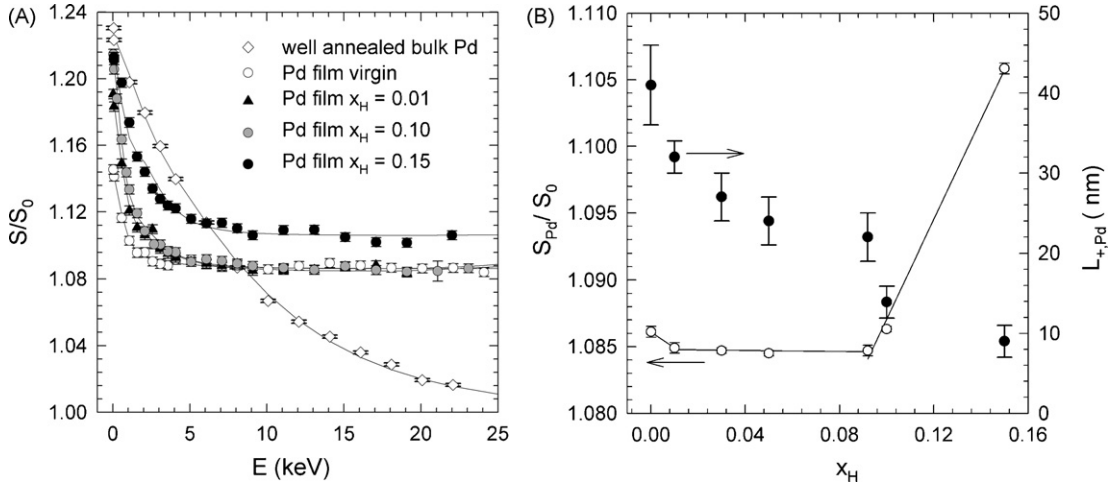

Fig. 2. (A) Selected $S(E)$ curves for the virgin film and the film loaded to various hydrogen concentrations. The solid lines show fits by the VEPFIT package. The $S(E)$ curve for well annealed bulk Pd reference specimens is plotted in the figure as well by open diamonds. (B) The S parameter S_{Pb} and the positron diffusion length $L_{+,Pd}$ for the Pd layer obtained from fits of the $S(E)$ curves as a function of hydrogen concentration. The solid lines in the figure represent a linear fit of S_{Pd} in the corresponding range of hydrogen concentrations.

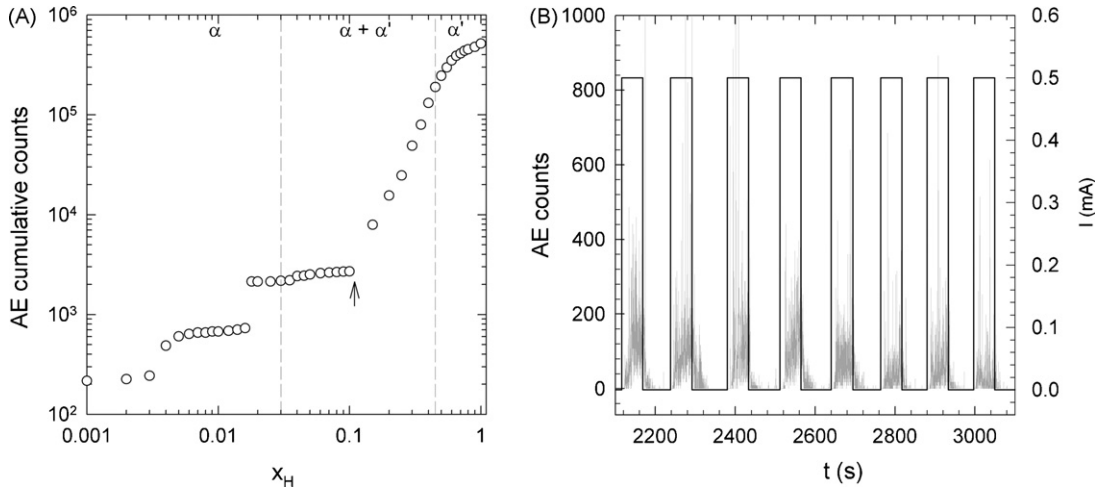

Fig. 3. (A) Dependence of the cumulative AE counts on hydrogen concentration. The dashed lines show the phase boundaries determined for the film. (B) Time chart showing simultaneously the detected AE counts and the loading current pulses during the step-by-step hydrogen charging in the concentration range $x_H > 0.1$, where buckling takes place.

concentrations ($x_H < 0.016$), hydrogen fills the open volume defects at grain boundaries. Hence, concentration of positron traps does not decrease, but local electron density in defects becomes higher and repulsive Coulomb interaction of trapped positron and hydrogen leads to reduced localization of positron wave function reflected by a decrease of S_{Pd}. A similar effect has been observed also in nanocrystalline Nb films [13]. At higher hydrogen concentrations, all the available deep traps at grain boundaries are filled and S_{Pd} becomes constant. A dramatic increase of S_{Pd}, accompanied by a drop of the positron diffusion length $L_{+,Pd}$, can be seen at $x_H \approx 0.10$. The occurrence of first buckles in the film was observed by OM at this concentration. At higher concentrations the number of buckles increases. Thus, the significant increase of S_{Pd} is due to positron trapping at new defects, most probably dislocations, introduced into the film by buckling.

A typical morphology of a buckle formed on the film is shown in Fig. 1b. The buckles occur straight sided, however, such straight-sided buckles can release the in-plane stresses only in one in-plane direction [5]. Therefore, at higher concentrations the straight buckles become wrinkled, and undulated shapes can be observed.

The cumulative AE counts are plotted in Fig. 3a as a function of hydrogen concentration. Obviously, the number of AE counts becomes to increase drastically at $x_H \approx 0.1$, where the buckling process starts. A lot of AE signals produced during buckling give an evidence for a collective movement of dislocations created during buckling of the film. A time chart of detected AE counts and time dependence of the applied current during the step-by-step hydrogen charging is shown in Fig. 3b. The time interval shown in the figure corresponds to the hydrogen concentration range above $x_H \approx 0.1$, i.e. the region where buckling takes place. One can clearly see that the AE bursts occur during the loading current pulse, i.e. during hydrogen insertion into the film. When the loading current is switched off, i.e. the film is not loaded anymore by hydrogen at this moment, also the AE counts disappear. This correlation demonstrates that the observed AE signals are generated by buckling of the film.

It should be noted that there is a small step-like increase in the cumulative AE count curve also at $x_H \approx 0.02$, i.e. prior to the onset of buckling. It could be due to the onset of plastic deformation in the loaded film. Thus, the film expands elastically up to $x_H \approx 0.02$, while above this concentration the stresses are released by plastic deformation. Since no increase of S_{Pd} was observed by SPIS at this concentration, the plastic deformation is realized most probably by sliding of nanocrystalline grains only, and not by creation of new defects.

X-ray diffraction studies and electrochemical potential measurements which will be published elsewhere [14] revealed that formation of the α′ phase in the film starts at $x_H \approx 0.03$ while the corresponding concentration for a bulk Pd single crystal is 0.017 only [15]. Thus, the film exhibits almost two times higher hydrogen solubility in the α phase. Similar narrowing of the miscibility gap was observed previously in nanocrystalline Pd [16] and can be explained by a high volume fraction of grain boundaries which contain open-volume defects and can accumulate more hydrogen than a regular lattice. The buckling takes place at the concentration range where the α and α′ phase co-exists in the film [17]. Formation of the α′ phase may also introduce new defects, but an increase of the defect density observed in the film is connected with the onset of buckling at $x_H \approx 0.1$ and not with the beginning of the α′ phase formation at $x_H \approx 0.03$.

4. Conclusions

Defect studies of hydrogen loaded nanocrystalline 1080-nm thick Pd film on sapphire substrate were performed in the present work. Positrons are trapped at vacancy-like open volume defects at grain boundaries already existing in the virgin film. Hydrogen is trapped at these open volume defects too. The hydrogen-induced compressive stresses cause buckling of the film at $x_H \geq 0.1$. It has been shown that dislocations are generated during the process of buckling which causes a significant increase of the S parameter and emission of bursts of AE signals during buckling.

Acknowledgements

Financial support from The Czech Science Foundation (project no. 202/05/0074), The Ministry of Education, Youth and Sports of The Czech Republic (project no. MS 0021620834) and The Alexander von Humboldt Foundation is highly acknowledged.

References

[1] U. Laudahn, A. Pundt, M. Bicker, U.V. Hülsen, U. Geyer, T. Wagner, R. Kirchheim, J. Alloys Compd. 293–295 (1999) 490.
[2] J. Colin, F. Cleymand, C. Coupeau, J. Grilhé, J. Philos. Mag. A 80 (2000) 2559.
[3] Y. Yu, C. Kim, S.C. Sanday, Thin Solid Films 196 (1991) 229.

[4] A. Pundt, P. Pekarski, Scr. Mater. 48 (2003) 419.
[5] A. Pundt, E. Nikitin, P. Pekarski, R. Kirchheim, Acta Mater. 52 (2004) 1579.
[6] A. Pundt, L. Brekerbohm, J. Niehues, P.J. Wilbrandt, E. Nikitin, Scr. Mater. 57 (2007) 889.
[7] R. Kircheim, Prog. Mater. Sci. 32 (1988) 261.
[8] W. Anwand, H.-R. Kissener, G. Brauer, Acta Phys. Pol. A 88 (1995) 7.
[9] A. van Veen, H. Schut, M. Clement, J. de Nijs, A. Kruseman, M. Ijpma, Appl. Surf. Sci. 85 (1995) 216.
[10] S.M. Myers, S.T. Picraux, R.E. Stolz, J. Appl. Phys. 50 (1981) 5710.
[11] J.K. Nørskov, F. Besenbacher, J. Bøttiger, B.B. Nielsen, A.A. Pisarev, Phys. Rev. Lett. 49 (1982) 49.
[12] P. Hautojärvi, H. Huomo, M. Puska, A. Vehanen, Phys. Rev. B 32 (1985) 4326.
[13] J. Čížek, I. Procházka, G. Brauer, W. Anwand, A. Mücklich, R. Kirchheim, A. Pundt, C. Bähtz, M. Knapp, Appl. Surf. Sci. 252 (2006) 3237.
[14] J. Čížek, I. Procházka, M. Vlach, N. Žaludová, G. Brauer, W. Anwand, A. Mücklich, R. Gemma, R. Kirchheim, A. Pundt, C. Bähtz, M. Knapp. J. Alloys Compd., submitted for publication.
[15] F.B. Manchster (Ed.), Phase, Diagrams of Binary Hydrogen Alloys, ASM International, Materials Park, 2000, p. 158.
[16] T. Mütschele, R. Kirchheim, Scr. Metall. 21 (1987) 1101.
[17] A. Pundt, R. Kirchheim, Annu. Rev. Mater. Res. 36 (2006) 555.